COBEM2015

ABCM Associação Brasileira de Engenharia e Ciências Mecânicas

23rd ABCM International Congress of Mechanical Engineering
December 6-11, 2015, Rio de Janeiro, RJ, Brazil

COMPOSITE LOW MODULE TU USE IN MECHANICAL UNIONS PINNED PRE TENSION, NO TENSION AND BONDED

Marcelo de Souza Marques
Tiago Soares Silva
Luiz Guilherme Meira Souza
Luiz Guilherme Vieira Meira de Souza
Mariana Lima de Oliveira
José Antônio Martins Neto
Universidade Federal do Rio Grande do Norte – UFRN, Av. Sen. Salgado Filho, 3000 - Lagoa Nova Natal - RN, 59078-970I
tiago_silva98@yahoo.com.br, marcelo.marques@ifrn.edu.br, lguilherme@dem.ufrn.br, lguilherme_souza@hotmail.com, marianalimagm@yahoo.com.br, josemartins@ifrn.edu.br

Abstract. *In recent years the joints mechanically bolted and glued has drawn the attention of the scientific community, the growth of its applications in various sectors of engineering. An advantageous feature of mechanical joints is the low sensitivity to surface preparation, service temperature or humidity. In parallel to the study of the joints mechanically fixed by screws, automotive and aerospace industries boosted the use of adhesives in glue joints in the assembly of structures, due to advantages such as better stress distribution, union capacity in different materials and reducing fatigue when compared to traditional methods of union. The strength of a glued joint are also influenced by various parameters; the thickness of the cord, the preparation of the adhering surface, the geometry of the joint, the type of glue used, the operating temperature and the humidity. The objective of this work is to extend the experimental study to investigate the influence of bolt preload on the failure modes compared to fixed together by pin without torque and compared with the resistance of a glued joint, used in laminated composites cotton reinforced with vegetable fibers. The applied preload moments were taken as 0 and 5 Nm concluded that the tensile failure mode either pure or combined, was present in all configurations of the joints pinned; the shortcomings of tension occurred in the samples submitted to the torque of 5.0 Nm in every relationship E/d the breaking load distribution in the composite gasket can be adjusted by varying some geometrical parameters of the sample.*

Keywords: *clearance, failure modes, maximum capacity, preload, geometry, momentum, articulate.*

1. INTRODUCTION

In recent years the joints mechanically bolted and glued has drawn the attention of the scientific community, the growth of its applications in various sectors of engineering. Especially by developing and designing a database is obtained through experimental data and analytical models, mostly are of empirical nature. An advantageous feature of mechanical joints is the low sensitivity to surface preparation, service temperature or humidity. In addition to allowing the removal in a greater number of times, without damaging the structure, careful selection of materials and geometric parameters becomes important to ensure the integrity and reliability of the structure. Especially by a bonding polymeric composite materials acting as a point of weakness and initiate a failure of the element at that point.

In parallel to the study of the joints mechanically fixed by screws, automotive and aerospace industries boosted the use of adhesives in glue joints in the assembly of structures, due to advantages such as better stress distribution, union capacity in different materials and reducing fatigue when compared to traditional methods of union. The strength of a glued joint are also influenced by various parameters; the thickness of the cord, the preparation of the adhering surface, the geometry of the joint, the type of glue used, the operating temperature and the humidity.

The objective of this work is to extend the experimental study to investigate the influence of bolt preload on the failure modes compared to fixed together by pin without torque and compared with the resistance of a glued joint, used in laminated composites cotton reinforced with vegetable fibers. The applied preload moments were taken as 0 and 5 Nm. In the experiment, during the process, the ratio of the distance from the edge and pin diameter (E/D) was changed from 1 to 4, while the relationship between the sample width and diameter of the pin (W/d) was constant at 4.

2. MATERIALS AND METHODS

Figure 1 shows the test sample. Their dimensions have been chosen according to Esendemir, 2011, and adapted to a width "W" fixed constant in order to maintain the relationship between the width of the sample and the pin diameter (W/d) for directing the focus of the study function a few settings.

Therefore: W = 25 mm; E = 5, 10, 15, 20 mm; L = 80 mm; D = 5.2 mm; d = 5 mm; t = 7.0 millimeters. Intentionally in this study there is a gap between the hole and the pin (bolt) of 3.84%, as the effect of slack second (Esendemir, 2011) is significant in the matter of crushing resistance in the design of mechanically fastened joints loaded. Furthermore, no backlash samples reach higher loading capacity. Therefore, the option to analyzing the worst conditions of loading. The clearance is defined by equation 1.

$$\lambda = \frac{\phi_{furo} \quad \phi_{pino}}{\phi_{furo}} \tag{1}$$

To develop the study, a laminated composite with the polyester resin matrix and vegetable cotton fabric was made up in the form of square plates with dimensions 250 cm x 250 cm x 7.5 mm. The plates were then cut with synthetic diamond disk, rectangles with dimensions shown in Figure 1.

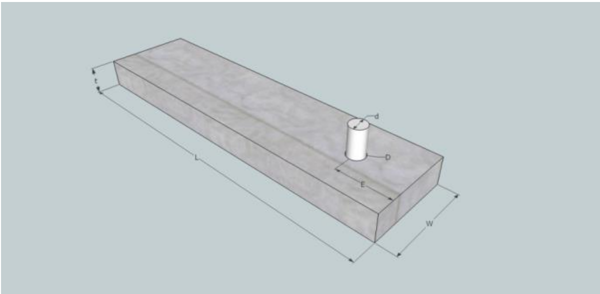

Figure 1. Test setup of pinned joint.

Each composite sheet was produced with nine bidirectional layers ($0/90^0$) balanced cotton plain fabric (density of 225.6 ± 12.40 g / m^2), and also arranged interspersed with orthophthalic polyester resin with 2% by weight MEK-P accelerator (methyl ethyl ketone). The mechanical properties of the laminates were determined by the authors by means of tensile testing. The average resistance to longitudinal traction corresponded to 31,38MPa. A single hard pin placed in the center hole, and a uniform tensile load P have been assigned to the sample. The tensile load is kept parallel to the model surface and symmetrical about the center line.

The geometry of the sticked joint is shown in Fig. 2. The laminates are adherent plates of 60 mm (length L_1), 25 mm (width W) and 7.0 mm (thickness) and are joined by a 25.0 mm overlap region (length L_2) and a region top. As adhesive was used orthophthalic polyester resin. To minimize rotation in the region of interest was chosen by the parallelism of the plates with membership area through the bonding job with overlapping and top joint. Was used in the experiments a torque wrench snap-1DF KING TONY 3426C, accuracy of ± 3% in accordance with DIN ISO 6789 and ASME B-10.14M - 2004 to obtain 5 Nm precharge time, screw with washer over circular hole (Figure 3).

Figure 2. Test piece with joint-adhesive ready for testing.

According Banea and Silva, 2009, the surfaces play an important role in the binding process interfering in the adhesive bonding of a group. The formation of a chemical bond in the appropriate surface is the most important step in the process of surface preparation, as a clean surface is a prerequisite for adhesion, but not a sufficient condition for durability.

Most structural adhesives works as a result of the formation of chemical bonds (mainly covalent) between the adhering surface atoms and the compounds which form the adhesive. These chemical bonds are the charge transfer mechanism between the adherends. Most failures in the adhesive bonding can be attributed to poor process during fabrication, lack of surface quality.

It was used in the traditional glued joint treatment recommended in the literature for thermoset composites, which includes abrasive / cleaning solvents. Trichloroethylene was used as a cleaning solvent and mechanical abrasion procedure was performed with sandpaper of different grain sizes (240, 400, 800, 1200), in descending scale roughness on the surface of the adherents to remove only a minimal layer of resin without exposing the fibers. The configuration of the apparatus for fixing the gasket is illustrated in Figure 3, the apparatus and subjecting the composite plate + the heads of the testing machine is shown in Figure 4.

Figure 3. Views of the fixing apparatus to fix the pinned joint in the testing machine.

Figure 4. Overview of the apparatus and the composite plate in the grips of the testing machine.

Wang, 2002 to consider the geometric dimensions of a sample as shown in Figure 1, defined the final tensions based on average tensions failure according to the equations:

Equation (2) the maximum bearing tension, $\sigma_b = \dfrac{P}{D.t}$

Equation (3) maximum tensile strength, $\sigma_T = \dfrac{P}{(W-D).t}$

Equation (4) maximum shear stress, $\tau_S = \dfrac{P}{2.E.t}$

Where P is the breaking load is taken as the maximum load obtained during tensile loading.

The composite was cured for 24 h at room temperature and under pressure of 1.0 MPa. Then, the holes were machined using half the cutting speed steel drill. Thus, a hole with 5.2 mm diameter was machined with a distance 'E' to the edge of the hole center, along the axis of symmetry, the dimensions chosen (E = 5, 10, 15 and 20 millimeters). The analysis of the failures were performed experimentally for nine different geometries.

All assays were performed with testing machine SHIMADZU AG - X, with 250 kN under temperature controlled cargo capacity at the Federal University of Materials Testing Laboratory of Rio Grande do Norte. The movement of the jaws is controlled by application of load at the rate of 0.5 mm / min. The test samples were rigidly attached to the testing machine. During the static tests, the load-displacement response was recorded by computer to the examination of the failure process in the bodies of damaged evidence. The tests were repeated five times for each configuration. The average values of the five tests in terms of maximum force was taken as the tensile strength.

3. RESULTS AND DISCUSSION

For the pinned joint was used geometrical parameter (E/d = 1, 2, 3, 4), due to the distance from the symmetry axis of the hole to the front face (E), the diameter pin, (d) and the difference in the configuration of the joint to make the comparison between the experimentally purpose of pre-load on the crushing strength and failure mode. Therefore, during the experimental process, a time used to pre-load the bolt 5 Nm for the four combinations of E/d and compared with four other combinations without preload.

A comparison with the strength of a glued joint was also raised. The pin diameter was 5 mm and the hole diameter 5.2 mm. Thus it was possible to observe the influence of preload on the board handily. As the shear strength of the pin was increased compared with the resistance of the pre-impregnated plate, the possibility of failure occurs is discarded due to the very low likelihood of failure.

The literature presents several failure modes for joining composite screws; four common modes are shown in Figure 5. The failure modes have been identified as drift, cleavage, shearing or cutting and rolling tension. Thus, depending on the ratios obtained E/d, it is possible to find cleavage failure modes, particularly if the fibers 0^0 are oriented or mixed modes of failure, especially when presented in pinnate together with clearance ratio $W/D \geq 3$.

For a bonded joint, Banea and Silva 2009 recognize that failure modes are determined by the quality of the connection on the interface to the geometry and the sample loading. And they should be characterized for a complete understanding of the adhesive properties and the joint to be investigated. In composite bonded joints of FRP materials in accordance with ASTM D5573, seven typical failure modes; adhesive failure, cohesive failure, cohesive failure thin layer, failure by tearing the fiber failure on small tear of the fiber failure by breaking the stem and joint failure. These modes are illustrated in Figure 6.

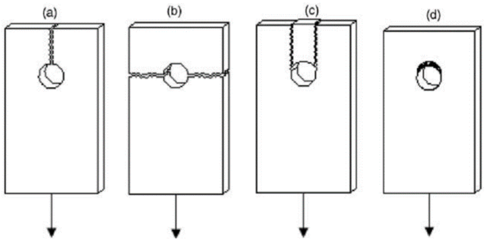

Figure 5. Common ways of failures in pinnate joints tests: (a) failure cleavage, (b) tensile failure; (c) fails by shearing, and (d) a bearing fault voltage (Sen et al., 2008).

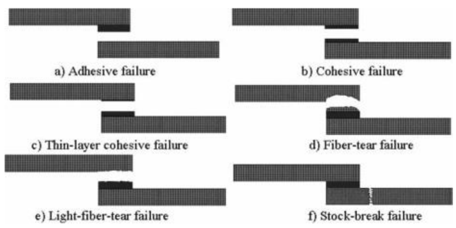

Figure 6. Possible modes of failure in bonded joints with adherent composite FRP (a) adhesive failure (b) cohesive failure (c) Thin layer cohesive failure (d) a tear flaw of the fiber, (e) failure small tear in the fiber, and (f) failure by breakage of the rod (Banea and Silva 2009).

Table 1. Modes of experimental failure for W / D = 5, no pre-load (0 Nm) and preload (5 Nm).

Ratio	**Failure Modes in joints**		
E/d	No torque 0 N	With torque 5 N	Bonded
1	C + T	C + T	CC + LF
2	T	T	
3	T + R	T	
4	T + R	T	

The mechanical joints fixed by pin, with and without tightening torque were compared keeping the relationship E/d of Table 1. Figure 7 show that there is dependence breaking load with respect to the torque applied on the screw joint.

It was noticed that in all ratios and/magnitude of the breaking load, in the joint bolt which is subjected to torque of 5 Nm, the joint is no greater than torque on the screw union. To compare the curve was plotted glued join in all the relations of Figure 7. As shown evidenced the lower load capacity for this configuration.

You can observe the discontinuity of loading on the glued joint between the members, that is characterized by the existence of cracks in the top surfaces that were attached (frontal areas adhered and broken by tensile stresses), as there is a butt joint of the break with displacement around 0.2 mm as the surface of the lap joint to resist loading, a new break point appears near the junction of 1.1 mm displacement (shear bond).

The failure mode on the bonded joint of a mixed fracture characteristics, ie the combination of cohesive fracture in a thin layer and fracture with small tear of the fiber. Thus have not been studied other settings for the glued joint, the reduced load capacity of this type of joint.

In samples 5 Nm of torque there was an increase in the maximum shift which occurred tensile strength, for example the sample of Figure 7 (c) reaches the sample with the largest torque load bearing capacity between 3.5 and 3.7 mm displacement, whereas the sample without tightening torque reaches the highest capacity in a region comprised between 2.7 to 3.0mm.

As can be seen in Figures 7 (b), (c) and (d) tensile failure mode is predominant, with Figure 7 (c) and (d) mixed with a small region in the samples failed by torque-free bearing, (0 Nm). However, in Figure 7 (a) shows almost the balance between cleavage and tensile failure.

Consequently, the time for pre charging is significant at the junction of resistance growth, since this increase in preload produces the appearance of frictional force, increasing the tensile strength of the sample.

Hibeler 2004 has demonstrated that when an axial force is applied to an element of a complex stress distribution at the load application point arises, and these voltage distributions complex also appear in the sections in which the cross-sectional area is changed. With an additional force of friction acting on the narrowing region of the cross section, new load distribution occur.

Thus the balance of power requires that the intensity of the resultant force developed by the stress distribution is equal to the load P. From the viewpoint of Materials Science, for polymer matrix composites, failure originates along the reinforcing fibers. It is therefore desirable to maximize high resistance interfacial resistance of the overall composite (Shackelford, 2008).

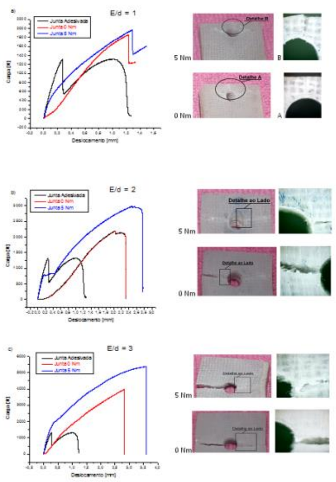

Figure 7. Comparison of bonded and pinnate together in samples with torque 0 Nm and 5 Nm.

The series of letters (a), (b), (c), (d) of Figure 8 represent the mean values of magnitudes; Bearing Voltage Maximum, Maximum Traction Tension, Stress Shear and Maximum Displacement Maximum Binding to loading, for different E / d in specimens with 0 Nm and 5 Nm of torque.

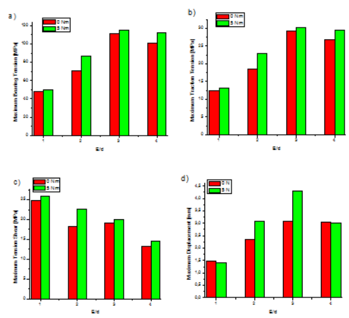

Figure 8. Stress Bearing, Traction, and Shear Displacement Maximum according to different relationships E / d for samples without torque (0 Nm) and torque (5 Nm).

In Figure 8 (a) the maximum bearing load did not behave linearly with respect to E / d, with the lowest value, E/d = 1 and 0 Nm of torque, 41.3% of the largest bearing tension. However, to E / d = 2 and d = 5 Nm of torque bearing tension reached 75.5% of the highest tension obtained, which was achieved in E / d = 3 and the sample subjected to torque of 5 Nm.

In all cases E / d, the samples with 5 Nm torque kept bearing tension above the samples with 0 Nm of torque. In (a), to E / d = 4 there was a decrease of 8.94% in the bearing together with the tension to 0 Nm and 2.5% for the joints with 5 Nm torque. It showed that crushing force gradually increased to higher values of the E / d, up to a limit where remained virtually constant.

The average of the maximum tensile strength is shown in Figure 8 (b), in which it realizes an increase of maximum tensile strength values from E / d = 1 to E / d = 3, not maintaining this growth for E / d = 4 in the samples with 0 Nm and 5 Nm of torque. It also became clearly explicit that the samples with 5 Nm of torque for any E / d, the value of maximum tensile stress was higher than the samples with 0 Nm of torque. For, according to equation (3), the maximum tensile strength for a fixed ratio W / d is proportional to the maximum breaking load "P" of the joint.

In Figure 8 (c) the behavior of the average of the maximum shear stress obtained by equation (4) decreases to values of E / d increased. So that the lower value found in E / d = 4 Nm of torque, corresponding to 51.2% of the maximum value belongs to the E / d = 1 to 5 Nm of torque.

The average displacement, in its maximum load at the joints, Figure 8 (d) proportional behavior obtained for the first three ratios E / d. However for E / d = 4, decreased by 32.3% compared to the larger displacement. However, for E / d = 1 there was little difference between the samples with 0 Nm of torque and 5 Nm of torque, corresponding respectively to 34% and 32.3% of the peak in displacement.

SEM images (TESCAN Equipment model VEGA 3 LMU the Czech Republic), surfaces of breaks in bonded joints and pinnate under maximum traction, cleavage and bearing the specimens with clearance subjected to maximum rupture load, (ie, "P") are shown in Figures 9-14.

Figure 9 shows the micrograph of self-adhesive surface with magnification 20X.

Figure 9. SEM micrograph of bonded surface.

Figure 9 (a), the bonded joint surface is photographed by a digital microscope at 20X magnification, where we can observe the border region of the two surfaces, showing depression on the glued area after rupture of the joint. Through the SEM in Figure 9 (b), we can see the peeling thin layer of adhesive, exposing the fibers and revealing tiny cracks in the matrix, caused by shear at the junction.

Figure 10 shows a micrograph of the inner surface of the hole, showing the crack cleavage.

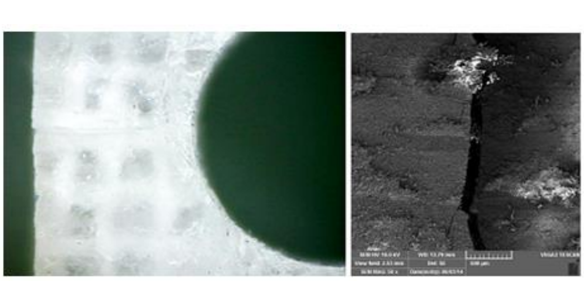

Figure 10. Micrograph of the inner surface of the hole, showing the crack cleavage.

The cleavage surface is shown in Figure 10 (a) and SEM image is extracted from Inner hole as seen in 10 (b), the damage occurs in the section completely. The crack is apparent in macro-scale separating the matrix material during crack propagation, characterized by the phenomenon of cracking in the matrix is that the occurrence of one or more cracks in the composite matrix. It was evident that a group of fibers was cut by the crack, causing a cohesive failure.

Figure 11 shows the tensile surface of the micrograph with magnification of 50X.

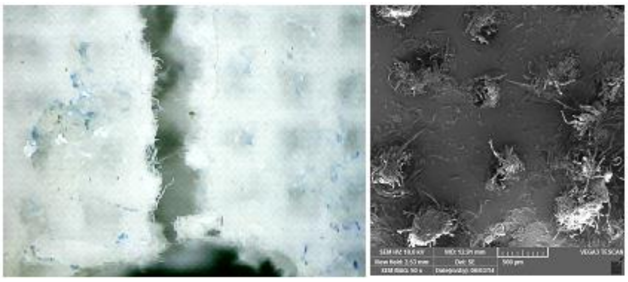

Figure 11. Traction surface micrograph.

Figure 11 (a) shows the region of fissuring in the fiber when a break occurs by the maximum tensile stress. It is observed that the composite fibers are oriented in the longitudinal direction of loading and contributed to the transfer of the matrix of tension for the dispersed phase. Separating these broken fibers corroborates break by transverse rupture. The SEM image in Figure 11 (b) shows a uniform distribution of the fibers in the matrix and good fiber-matrix interactions, as the fiber was broken closest to the array surface. This demonstrates the breaking of them and not their homelessness.

Figure 12 shows a micrograph of the surface tension of the SEM, showing the structure of cellulose fibers consists of crystalline and amorphous regions.

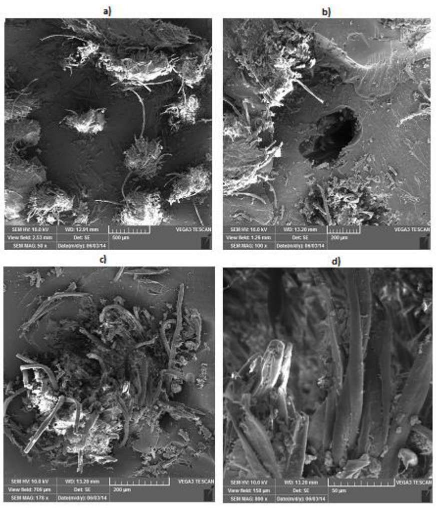

Figure 12. Traction surface of the SEM micrograph.

In Figure 12 (a) - (d) it is observed that there are no voids between the fibers and the matrix but also the number of the drawn fiber array (fiber pullout) is low. This behavior is characteristic of composites with good interaction between components and is responsible for promoting usually a good transfer tensile set between the fiber-matrix.

Figure 13 shows a photograph by a digital microscope (20X) of the bearing surface.

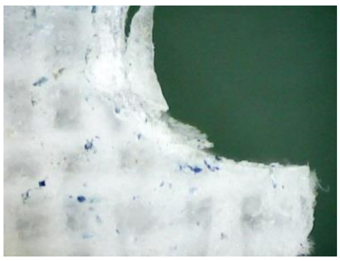

Figure 13. Photograph by digital microscope (20X) of the bearing surface.

Figure 13 shows a small surface for bearing failure. It can be seen in this figure that the crushing occurs in the matrix material when a force is applied by the pin and the crack occur in some areas of the matrix material. This type of loading can allow large cracks and narrow, with perpendicular to the direction of the applied force.

4. CONCLUSIONS

The main objective is the prevention of failure load and determining the failure modes of the joints fixed with torque without torque and pasted, studying the influence of the geometry of mechanical linkage when subjected to static loads controlled. The use of scanning electron microscopy was used to investigate the damage to broken surfaces of the samples. Through the experimental results and analysis using the scanning electron microscopy was concluded.

1. Comparison of tensile strength of the single joint configuration bonded with other variations of geometries together pinnate showed a value below the lower rupture load found for pinnate junction;
2. The tensile failure mode either pure or combined, was present in all configurations of pinnate together;
3. The main failure of tension occurred in the samples submitted to the torque of 5.0 Nm in every relationship E / d;
4. The distribution of the rupture load the composite board can be changed by varying some geometric parameters of the sample;
5. For the E / d = 1, the mixed-mode failure cleavage + traction occurred to pinnate junction with 0 Nm of torque and 5 Nm However, there was a predominance of cleavage as the main cause of the collapse of the joint;
6. Except in the smallest ratio E / d the tensile failure mode was not directly responsible for the joint rupture or subjected to torque 5.0 Nm or not;
7. The breaking load, while charging by pulling the junction, influences the failure modes;
8. Was noticed that the fibers are broken in the direction perpendicular to the applied load under tensile stress in the sample;
9. During cleavage the matrix material is accumulated in the longitudinal direction of the fibers and loses its adhesive property;
10. While charging the bearing stresses produced crushing of the material in contact with the pin in the joint.

5. REFERENCES

Angélico, R. A., Ribeiro, M. L., Silvestrini, R. H., Di Salvo,F. E. J. e Tita, V. (2010). Investigação do Comportamento Mecânica de Junções de Compósitos Termoplásticos, VI Congresso Nacional de Engenharia Mecânica.

Banea, M. D. e Silva, L. F. M. (2009). Adhesively bonded joints in composite materials: An overview, Proceedings of the Institution of Mechanical Engineers, Part L: Journal of Materials Design and Applications 2009 223: 1

Esendemir, U¨. (2008). Failure Analysis of Woven Glass-Epoxy Prepreg Bolted Joints Under Different Clamping Moments, Advanced Composite Letters, 17: 165-175.

Esendemir, U¨. (2011). An Experimental Study of Mechanically Fastened Composite Joints with Clearance, International Journal of Damage Mechanics, 1–17.

Gere, J. M., Goodno, B. J. (2010). Mecânica dos Materiais. 7 ª ed. São Paulo: Cengage Learning, 2010. 858p.

Hibeler, R.C. (2004). Resistência dos Materiais. 5ª ed. São Paulo: Prentice Hall Brasil, 2004. 585p.

Kumar, R.L. V., Bhat, M.R., e Murthy, C.R.L. (2013). Experimental Analysis of Composite Single-lap Joints Using Digital Image Correlation and Comparison with Theoretical Models, Journal of Reinforced Plastics and Composites 32(23) 1858–1876.

Lokensgard, E. (2013). Plásticos Industriais: Teoria e Aplicações. Tradução da 7 ed. São Paulo: Cengage Learning, 2013. 616p.

Molitor, P., Barron, V. and Young, T. (2001). Surface Treatment of Titanium for Adhesive Bonding to Polymer Composites: A Review, International Journal of Adhesion and Adhesives, 21(2): 129–36.

Reis, P. N.B., Ferreira, J. M. e Richardson, M. O. W. (2012). Effect of the Surface Preparation on PP Reinforced Glass Fiber Adhesive Lap Joints Strength, Journal of Thermoplastic Composite Materials, 25: February 2012

Sen, F., Sayman, O., Özcan, R., and Siyahkoc¸, R. (2010). Failure Response of Single Bolted Composite Joints Under Various Preload, Indian Journal of Engineering & Materials Science, 17: 39-48.

Shackelford, J.F. (2008). Introdução à Ciência dos Materiais para Engenheiros. 6ª Ed. São Paulo: Pearson Prentice Hall Brasil, 2008. 556p.

Thoppul, S.D., Finegan, J. and Gibson, R.F. (2009). Mechanics of Mechanically Fastened Joints in Polymer-Matrix Composite Structures _a Review, Composite Science and Technology, 69: 301-329.

Wang, Y. (2002). Bearing Behavior of Joints in Pultruded Composites, Journal of Composite Materials, 36: 2199-2216.

6. RESPONSIBILITY NOTICE

The author(s) is (are) the only responsible for the printed material included in this paper.